Corrosion of Copper-Coated Steel Containers for Long-Term Used Nuclear Fuel Storage

D.S. Hall[1], S. Ramamurthy[2], T. Standish[3], V. Dehnavi[3], D. Zagidulin[3], J. Chen[3], R.L. Jacklin[2],P.Keech[1], and D.W. Shoesmith[2,3]

[1]Nuclear Waste Management Organization, Toronto, Ontario, Canada
[2]Surface Science Western, The University of Western Ontario, London, Ontario, Canada
[3]Department of Chemistry, The University of Western Ontario, London, Ontario, Canada

pkeech@nwmo.ca, sramamur@uwo.ca, twells3@uwo.ca, vdehnavi@uwo.ca, dzagidul@uwo.ca, jchen496@uwo.ca, rebecca.jacklin@uwo.ca, dhall@nwmo.ca, dwshoesm@uwo.ca

Abstract

Copper-coated steel containers are currently considered by the Nuclear Waste Management Organization (NWMO) for the long-term storage of used nuclear fuel. NWMO has conducted extensive investigation of various techniques for coating copper on steel and the feasibility of coating very large cylindrical steel containers (> 2 m long and ~ 0.5 m in diameter). The results from their investigation have allowed NWMO to identify two preferred coating methodologies: namely electrodeposition for the container prior to being loaded with used nuclear fuel, and cold spray for covering the closure weld of a filled container at a packaging facility. Considering that these containers will be housed in deep geological repositories (DGRs) for many thousands of years, their long-term corrosion performance is one of the potential life limiting factors. Of particular interest is the comparison of the corrosion behaviour of the copper coating to that of the wrought copper for which extensive data is available in the literature.

Differences in the properties of the two coatings were determined in the as-received condition (top down) and after preparing polished cross-sections. Long-term electrochemical experiments were performed on annealed cold spray (CSA), electrodeposited (ED) and SKB wrought copper (SKB) samples under different redox conditions for a period of 150 days or greater. Additional samples placed in the bottom of the cell were used to determine the evolution of the surface oxide composition as a function of the immersion time. The results from these measurements indicate that there is no significant difference in the corrosion behavior of the CSA and ED samples and that their corrosion behaviour was similar to that of the SKB copper. In addition, the oxide composition is also similar for the samples examined in this study and is consistent with the expected composition under different exposure conditions.

1. Introduction

The internationally accepted method for the long-term disposal of nuclear fuel waste is permanent storage in a deep geological repository (DGR). The list of nations currently considering DGRs includes Belgium, Canada, China, Finland, France, Germany, Japan, South Korea, Russia, Spain, Sweden, Switzerland, and the United Kingdom. A key component of the DGR design is the use of multiple engineered and natural barriers to isolate the fuel from the environment, minimizing long-term safety and environmental risks (Figure 1) [1]. A major component of this design is the UFC, which must be strong enough to withstand geological pressures, including the additional load during any glaciation events, and chemically resistant to long-term corrosion.

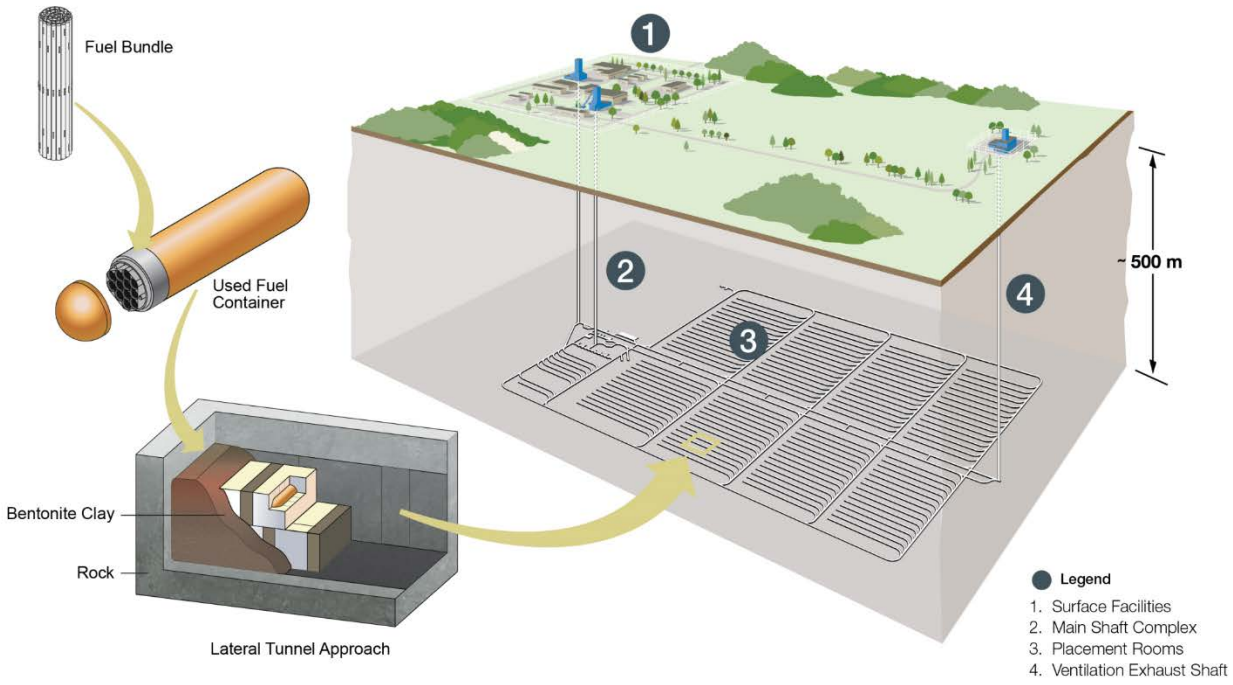

Figure 1The proposed multiple barrier system in a Canadian deep geological repository, showing the NWMO Mark 2 used fuel container.

Copper has been under consideration as a corrosion-resistant material for UFCs since the 1970s, when DGR research and development began. Copper was originally chosen for its thermodynamic stability under predicted DGR conditions, a choice that has since been supported by decades of corrosion research and the analysis of archaeological samples where metallic copper has remained intact in the earth for centuries [2,3]. In the case of a Canadian DGR, the most recently evaluated corrosion allowance for all the processes that significantly affect copper materials is 1.3 mm as the conservative maximum after one million years of storage [4,5]. That is, it is expected that much less than 1.3 mm of copper will actually corrode over this time period.

Sweden and Finland have proposed a ‘dual-vessel’ container (KBS-3, Figure 2a) that would consist of a large cast-iron inner vessel for structural strength and a 50 mm thick cylindrical copper ‘overpack’ for corrosion resistance [6]. The filled UFC would be over 4 m long, 1 m in diameter, and would weigh over 25 t. Canada has also developed a “Mark 1” dual-vessel container design (Figure 2b), where an inner steel cylinder is suggested in place of a honeycomb cast-iron insert. This difference arises because, unlike the Scandinavian power plants, CANDU reactors use small, natural uranium fuel bundles that can be packed very closely together without risk of reaching criticality. Because of manufacturing considerations, the dual-vessel designs use far more copper (~50 mm) than is necessary for corrosion resistance in a Canadian DGR (< 1.3 mm).

In recent years, NWMO has designed a new container geometry that is optimized for storing CANDU fuel bundles (Figure 2c). Consisting of two hemi-spherical heads welded to a cylindrical body, the NWMO Mark 2 UFC is just 2.5 m in length, 0.57 m in diameter and will weigh less than 3 t when filled [7]. The decreased dimensions and weight will significantly simplify the handling and transportation of filled containers. Another key advance in this design is the use of modern coating technologies to apply a 3mm corrosion-resistant copper layer directly onto the surface of the carbon-

steel core. NWMO has identified two preferred coating methodologies; electrodeposition for the empty containers and lids prior to loading, and cold spray for covering the closure welds of filled containers [8]. Despite the much thinner coating, the copper layer still significantly exceeds the necessary corrosion allowance[5]. This design also eliminates the concerns faced by dual-vessel UFCs over creep ductility degradation and, therefore, the need for phosphorus doping [6,7,9].

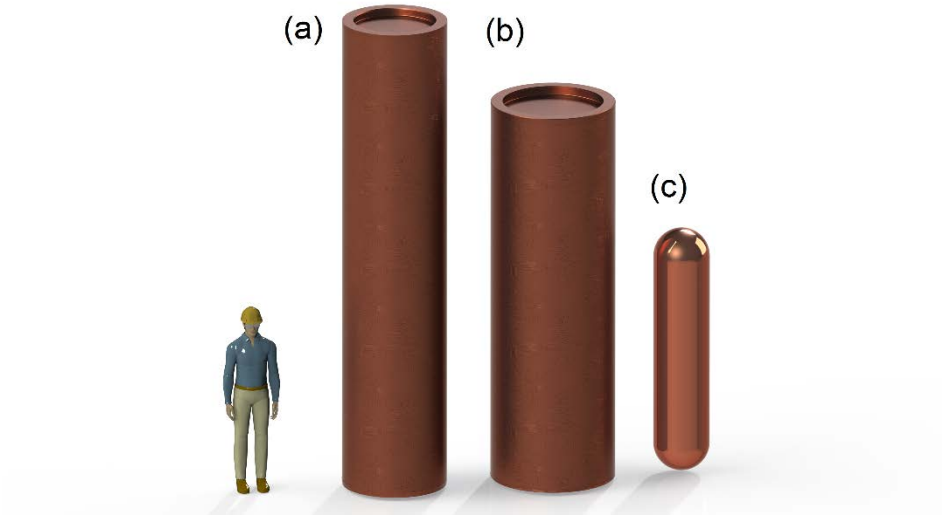

Figure 2 Comparison of the a) KBS-3, b) NWMO Mark 1 and c) NWMO Mark 2 used fuel container designs. The newest design is optimized for CANDU fuel bundles and applies modern coating techniques to significantly decrease the amount of copper required.

This work examines the properties of electrodeposited (ED) and annealed cold spray (CSA) copper coatings on carbon-steel, as well as their corrosion performance. Of particular interest is the comparison of the corrosion behaviour of the copper coatings to that of the Swedish Nuclear Fuel and Waste Management Company's phosphorus-doped, oxygen-free wrought copper (SKB) for which extensive data is available in the literature. Samples were examined as-received and after long-term corrosion testing in various redox conditions.

2. Experimental Methods

2.1 Sample Preparation

Integran Technologies Inc. (Mississauga, Ontario) supplied copper-coated mild steel samples formed by electrodeposition (ED) from a Cu(II) solution [10,11]. Although the exact details are proprietary, it is known that the bath contained pyrophosphate constituents to achieve high copper purity. A pulsed electrodeposition method was followed by a surface treatment to remove slight surface roughness. The resulting coatings are ~ 3 mm thick.

Cold spray samples (CSA) were prepared by the Surface Technologies Group (Advanced Forming and Coatings Division) at the Industrial Materials Institute of National Research Council Canada (NRC, Boucherville, Québec) [12,13]. Commercially available low-oxygen copper powder was deposited on grit-blasted steel substrates using a PCS-800 system (Plasma Giken Co. Ltd., Toshima-ku, Tokyo, Japan). He and N_2 were used as the accelerant gases for the bond coat and subsequent

coats, respectively. A bond coat is required to obtain good adhesion of the copper on the steel substrate [13]. The samples in this work were annealed for 1 h at 350 °C in an argon atmosphere.

Phosphorus-doped, oxygen-free wrought copper specimens (SKB) were supplied by the Swedish Nuclear Waste and Fuel Management Company (≥ 99.99% Cu, Stockholm, Sweden).

Specimens were polished on all sides using SiC paper (lubricated with water) and then a 3 μm diamond paste suspension (lubricated with Varsol). For the samples monitored electrochemically, a steel wire was soldered to the back of the sample and then covered with heat-shrinking Teflon. The specimens were coated with Amercoat™ on all sides except one, and cured in an oven at 60 °C for 24 h. The exposed face was then further polished using a 3 μm diamond paste (lubricated with Varsol). Where applicable, through-coating defects were simulated by drilling a 0.5 mm diameter hole to expose the underlying copper/steel interface (Figure 3a). The sample was then cleaned by sonication in methanol and coated with Amercoat™ such that only the top copper face was exposed; i.e., the face with the hole drilled in it (Figure 3b). The exposed face was wet-polished with SiC paper (2400 grit) and water, rinsed with methanol and dried in a stream of argon gas.

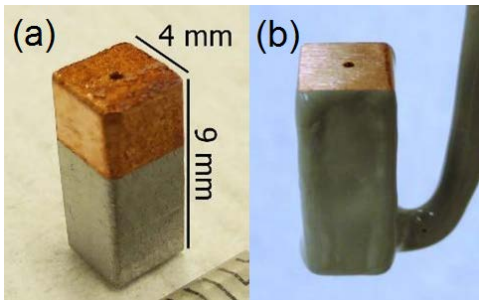

Figure 3 (a) A through-coating defect was simulated by drilling a hole until the underlying steel was exposed. (b) The sample was connected to a wire current collector and coated such that only the top copper face was exposed.

2.2 Surface and Materials Analysis

Surface imaging and elemental analysis were measured with a Hitachi S-4500 field emission scanning electron microscope (SEM) equipped with a Quartz XOne energy dispersive X-ray spectroscopy (EDX) system. Raman spectra were collected with a Renishaw model 1000 spectrometer equipped with a Melles Griot 35 mWHeNe laser (λ = 632.8 nm) that produces a focused beam ~2 μm in diameter at the sample surface.

2.3 Corrosion and Electrochemical Testing

Electrochemical measurements were performed in a standard three-electrode Pyrex cell using a saturated calomel electrode (SCE) as the reference and Pt foil as the counter electrode. Corrosion potential (E_{corr}) and linear polarization resistance (R_p) measurements were collected with Solartronpotentiostats and Corrware softwareversion 3.2 or 3.3. Experiments were conducted in 3 mol L^{-1}NaCl solution, prepared with high purity de-ionized water (MilliQ, 18.2 MΩ cm) and high purity NaCl (99.999 %), that was purged with high purity oxygen or argon, on the benchtop, or in an anaerobic glove box. Long-term electrochemical experiments were performed on CSA, ED, and SKB samples exposed to a 3 mol L^{-1}NaCl solution for ≥ 150 days.

3. Results and Discussion

3.1 Corrosion in Anoxic Solution

The copper coated-steel samples ED, CSA, and SKB were immersed in an oxygen-free (≤ 0.042 ppb [14]), 3 mol L^{-1}NaCl aqueous solution, stored in an anaerobic glove box. The corrosion potential, E_{corr}, and the linear polarization resistance, R_p, were measured for several months (Figure 4), with similar results for all three samples. The corrosion potential quickly reached a stable value and remained approximately within the range -375 to -380 mV_{SCE}. This potential window is consistent with the reported range for copper in anaerobic chloride solution[15,16]. In contrast, $R_p$initially decreased slightly and then slowly increased to nearly 10 times the minimum value. The resistance of the SKB electrode was the greatest, ~2 times that of the other two samples, which were comparable with one another. Because the samples were prepared identically, including the polishing regime, this difference is not attributable to surface roughness effects.

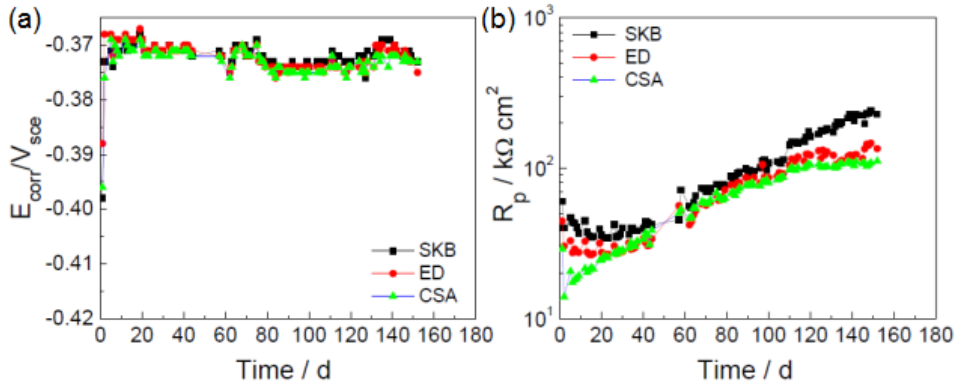

Figure 4 The evolution of the (a) corrosion potential and (b) linear polarization resistance on ED, CSA, and SKB electrodes stored in anoxic 3 mol $L^{-1}NaCl_{(aq)}$.

Despite the observed changes in R_p, optical micrographs show no visible indication of copper corrosion for any of the samples (Figure 5, top and middle rows). The SEM micrographs (Figure 5, bottom row), however, reveal the presence of a small amount of crystalline deposit on the electrode surfaces. EDX and Raman analyses indicate that this crystalline product is Cu_2S, which commonly forms in sulfide-containing solutions [17,18]. Trace bisulfide impurities are introduced in high purity NaClfrom the purification process used to remove heavy metal cations. The changes in R_p over time are therefore attributed to the slow reaction of bisulfide anions with the air-formed surface oxide. At first, the oxide was removed, causing the initial decrease in R_p:

$$Cu_2O + SH^- \rightarrow Cu_2S + OH^-$$

Following removal of the oxide, the underlying metal reacted withbisulfide, slowly increasingR_p:

$$Cu + 2\,SH^- \rightarrow Cu_2S + S^{2-} + H_2$$

This latter reaction is quite rapid and is expected to have been limited by the slow diffusion of trace bisulfide to the electrode surfaces [19].

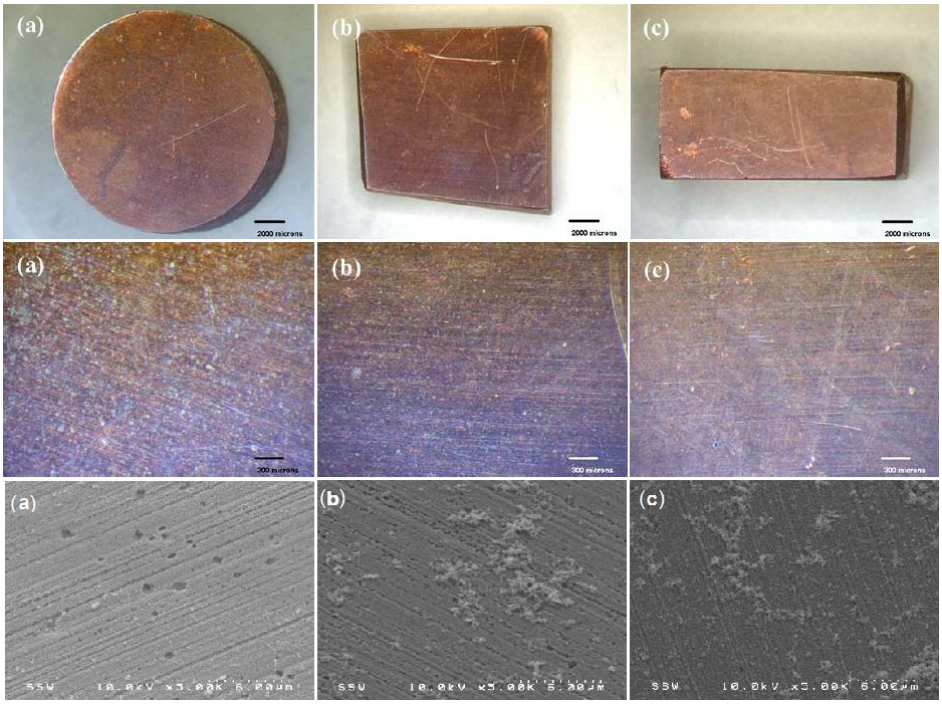

Figure 5 Optical (top and middle rows) and SEM (bottom row) micrographs of the (a) CSA, (b) ED, and (c) SKB electrodes following storage in anoxic 3 mol $L^{-1}NaCl_{(aq)}$.

3.2 Corrosion in Oxygenated Solution

Although a DGR will be anoxic over the long term, there is an initial oxygen-rich period during and immediately following the emplacement of the fuel waste before the anoxic condition will be established. Therefore, the above experiment was repeated, except that the solution was instead purged with a flow of O_2 for the first 61 days, and then the switch to anoxic conditions was simulated by replacing the purge gas with argon. During the initial oxic period (*i.e.*, while oxygen was bubbled into the solution), E_{corr} increased from -320 mV_{SCE} to a maximum of approximately -170 mV_{SCE} (Figure 6a). This increase in E_{corr} coincided with the visible accumulation of green solid on the electrodes (Figure 7, upper row). The value of E_{corr} was unstable, decreasing when the corrosion product occasionally fell off the electrodes and increasing as it was replaced by further corrosion and corrosion product build up.The R_p supports this observation, where it increased as the electrode was presumed to be covered in corrosion deposit and decreased as the underlying metal was exposed by deposit delamination events (Figure 6b). SEM micrographs (Figure 7, lower row), accompanied by EDX surface analysis, indicate that the corrosion deposits are the same species on all three electrodes. X-ray diffraction identified that this material is atacamite, $Cu_2(OH)_3Cl$, the expected product of copper corrosion in aerated chloride solutions [20]. Therefore, the corrosion behaviour of the two copper coatings in oxygenated solutions is very similar to that of the SKB wrought copper.

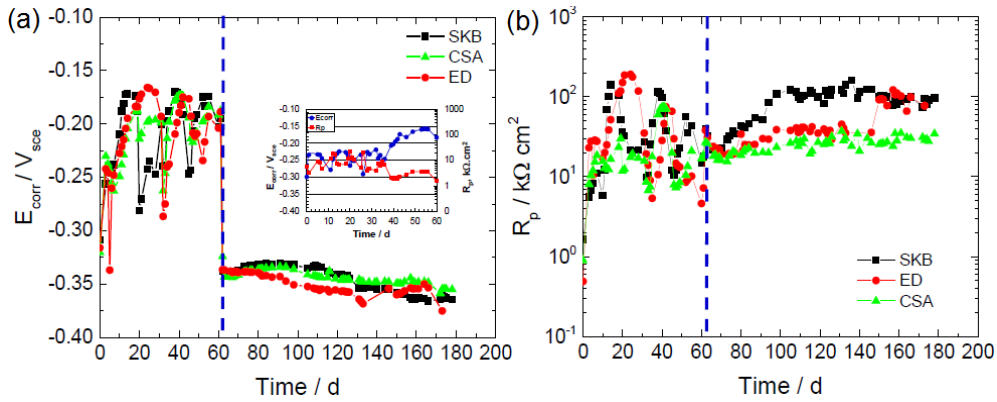

Figure 6The evolution of the (a) corrosion potential and (b) linear polarization resistance on ED, CSA, and SKB electrodes stored in 3 mol $L^{-1}NaCl_{(aq)}$. O_2 was bubbled through the solution for 61 d (oxic). The solution was then purged with argon, indicated by the vertical dashed lines (anoxic).

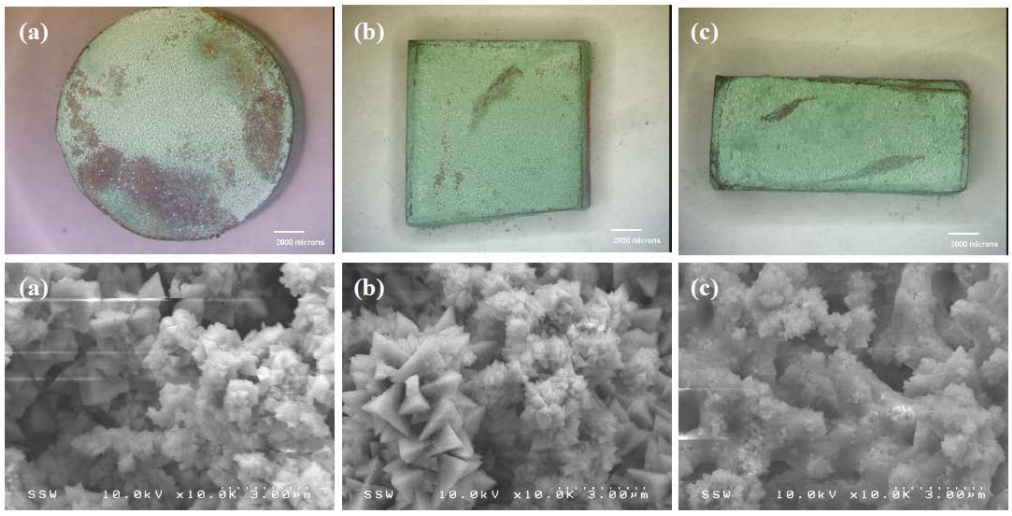

Figure 7 Optical (upper) and SEM (lower) micrographs of the (a) CSA, (b) ED, and (c) SKB samples following storage in oxygenated 3 mol $L^{-1}NaCl_{(aq)}$ for 61 days.

As the solution was deaerated with argon, E_{corr} quickly decreased to -340 mV_{SCE} and then gradually to the range -375 to -350 mV_{SCE}. This is consistent with the potential range measured above for copper in anoxic chloride solution (Figure 4a). Again, the corrosion behaviour of the copper coatings is similar to that of the SKB wrought copper.

3.3 Through-Defect Corrosion

A CSA sample with a simulated through-defect was immersed in O_2-purged 3 mol $L^{-1}NaCl_{(aq)}$ solution for 24 h. Red-brown corrosion deposit visible at the perimeter of the defect surface (Figure 8a) was identified by Raman to contain goethite (α-FeOOH), akaganeite (β-FeOOH), and lepidocrocite (γ-FeOOH), as shown in Figure 8b[21,22]. The sample was then cross-sectioned and imaged by SEM (Figure 8c). There is corrosion deposit visible at the base of the through-defect, identified by Raman spectroscopy as primarily maghemite (γ-Fe_2O_3), whereas the corrosion product elsewhere in the defect is primarily goethite, akaganeite, and lepidocrocite (Figure 8d)[21]. This suggests that the O_2 concentration is limited at the base of the defect, based on the lower oxygen-to-iron ratio.

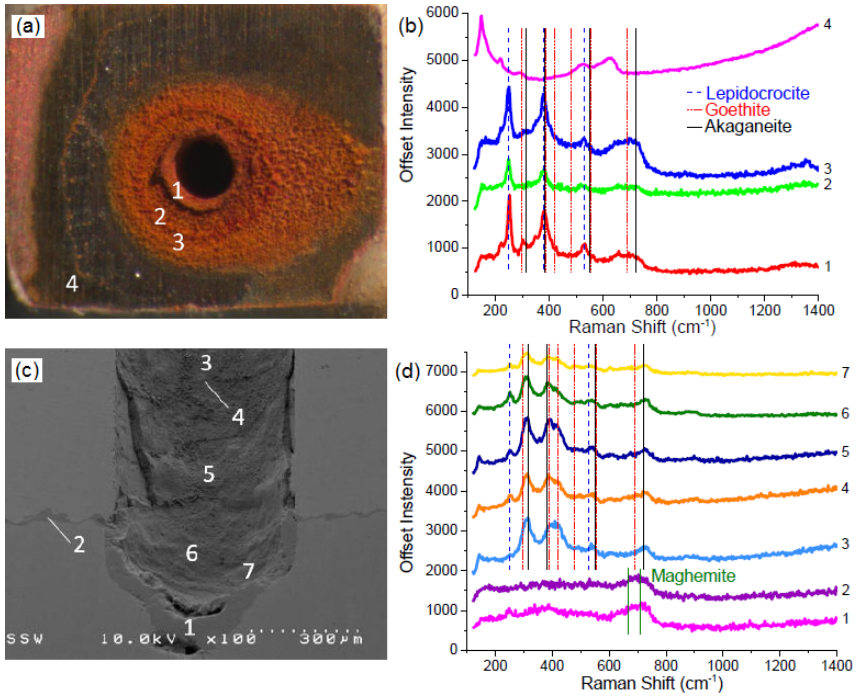

Figure 8 The through-defect sample was analyzed following corrosion: (a) Optical image of the top copper surface, (b) Raman spectra recorded at the numbered locations on the optical image, (c) SEM of the cross-sectioned sample, and (d) Raman spectra recorded at the numbered locations on the SEM micrograph.

A basic scheme is proposed for the physical and chemical processes during through-defect corrosion (Figure 9).Oxygen reduction on the bold copper surface drives the oxidative dissolution of iron at the defect base. As the dissolved iron(II) cations diffuse up the defect, direct oxidation with O_2 forms precipitate along the defect wall and at the electrode surface. SEM and Raman (Figure 8d), indicate that maghemite is deposited along the copper/steel interface[21]. Further studies are ongoing to assess the extent and severity of the propagation along this interface. However, this may indicate a need to couple further corrosion measurements with the ongoing optimization of the copper steel adhesion for cold-sprayed coatings.

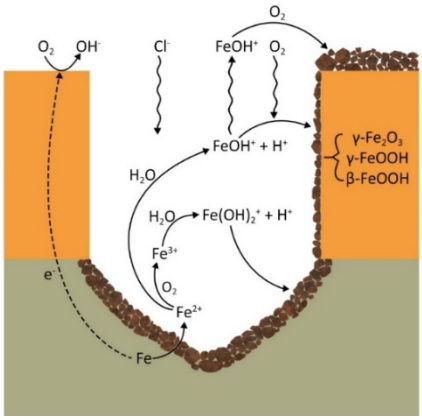

Figure 9 The chemistry of a corroding through-defect in oxygenated 3 mol L^{-1}NaCl solution.

4. Conclusions

The corrosion behaviour was compared for electrodeposited, cold-sprayed, and wrought copper samples in anoxic and oxygenated aqueous chloride solutions. In general, the corrosion behaviour of all three materials is similar. Under anoxic conditions, the only detectable corrosion was due to trace bisulfide impurities in the NaCl, which lead to Cu_2S formation. In oxygenated solution, the corrosion reactions were mass-transport limited and deposited atacamite, $Cu_2(OH)_3Cl$, on the sample surfaces. Exposure of a simulated through-defect to oxygenated chloride solution created a galvanic couple between oxygen reduction on the bold copper surface and iron dissolution at the bottom of the defect. Direct oxidation of the dissolved Fe(II) cations produced various FeOOH species along the defect wall and on the electrode surface. Corrosion occurred along the copper/steel interface. Future work will examine whether modifications to the cold spray procedure to improve the copper-steel adhesion suppress this localized corrosion.

5. Acknowledgements

The authors gratefully acknowledge assistance provided by personnel at Western University's Physics and Engineering machine shops and Department of Chemistry, and Surface Science Western. This research was funded by the Nuclear Waste Management Organization (NWMO, Toronto, Canada).

6. References

[1] F. Garisto, T. Kempe, P. Gierszewski, Technical Summary of the Safety Aspects of the Deep Geological, NWMO TR-2009-12, Nuclear Waste Management Organization, Toronto, Canada, 2009.

[2] M.L. Chastain, A.C. Deymier-Black, J.E. Kelly, J.A. Brown, D.C. Dunand, Metallurgical analysis of copper artifacts from Cahokia, J. Archaeol. Sci. 38 (2011) 1727–1736. doi:10.1016/j.jas.2011.03.004.

[3] F. King, A natural analogue for the long-term corrosion of copper nuclear waste containers—reanalysis of a study of a bronze cannon, Appl. Geochem. 10 (1995) 477–487. doi:10.1016/0883-2927(95)00019-G.

[4] G.M. Kwong, Status of Corrosion Studies for Copper Used Fuel Containers Under Low Salinity Conditions, NWMO TR-2011-14, Nuclear Waste Management Organization, Toronto, Canada, 2011.

[5] J.R. Scully, M. Edwards, Review of the NWMO Copper Corrosion Allowance, NWMO TR-2013-04, Nuclear Waste Management Organization, Toronto, Canada, 2013.

[6] Design and production of the KBS‑3 repository, SKB TR-10-12, SvenskKärnbränslehantering AB, Stockholm, Sweden, 2010.

[7] C.H. Boyle, S.A. Meguid, Mechanical performance of integrally bonded copper coatings for the long term disposal of used nuclear fuel, Nucl. Eng. Des. 293 (2015) 403–412. doi:10.1016/j.nucengdes.2015.08.011.

[8] P.G. Keech, P. Vo, S. Ramamurthy, J. Chen, R. Jacklin, D.W. Shoesmith, Design and development of copper coatings for long term storage of used nuclear fuel, Corros. Eng. Sci. Technol. 49 (2014) 425–430. doi:10.1179/1743278214Y.0000000206.

[9] R. Sandström, H.C.M. Andersson, The effect of phosphorus on creep in copper, J. Nucl. Mater. 372 (2008) 66–75. doi:10.1016/j.jnucmat.2007.02.004.

[10] K. Aust, I. Brooks, F. Gonzalez, P. Lin, G. Palumbo, K. Tomantschger, N. Nagarajan, Method for preparing polycrystalline structures having improved mechanical and physical properties, CA 2674403, 2012.

[11] P.G. Keech, P. Lin, N. Mahalanobis, Electrodeposited copper coatings for used fuel containers, in: 35th Annual CNS Conference Proceedings, Canadian Nuclear Society, Saint John, Canada, 2015.

[12] P. Jakupi, P.G. Keech, I. Barker, S. Ramamurthy, R.L. Jacklin, D.W. Shoesmith, D.E. Moser, Characterization of commercially cold sprayed copper coatings and determination of the effects of impacting copper powder velocities, J. Nucl. Mater. 466 (2015) 1–11. doi:10.1016/j.jnucmat.2015.07.001.

[13] P. Vo, D. Poirier, J.-G. Legoux, P.G. Keech, Application of Copper Coatings onto Used Fuel Canisters for the Canadian Nuclear Industry, in: J. Karthikeyan, C. Kay (Eds.), High Pressure Cold Spray: Principlesand Applications, ASM International, 2016.

[14] R. Partovi-Nia, S. Ramamurthy, D. Zagidulin, J. Chen, R. Jacklin, P. Keech, D.W. Shoesmith, Corrosion of Cold Spray Deposited Copper Coating on Steel Substrates, Corrosion. 71 (2015) 1237–1247. doi:10.5006/1757.

[15] F. King, C.D. Litke, M.J. Quinn, D.M. LeNeveu, The measurement and prediction of the corrosion potential of copper in chloride solutions as a function of oxygen concentration and mass-transfer coefficient, Corros. Sci. 37 (1995) 833–851. doi:10.1016/0010-938X(95)80013-1.

[16] F. King, C. Lilja, K. Pedersen, P. Pitkanen, An update of the state-of-the-art report on the corrosion of copper under expected conditions in a deep geologic repository, SKB TR-10-67, SvenskKärnbränslehantering AB, 2010.

[17] J. Chen, Z. Qin, D.W. Shoesmith, Kinetics of Corrosion Film Growth on Copper in Neutral Chloride Solutions Containing Small Concentrations of Sulfide, J. Electrochem. Soc. 157 (2010) C338–C345. doi:10.1149/1.3478570.

[18] J.M. Smith, J.C. Wren, M. Odziemkowski, D.W. Shoesmith, The Electrochemical Response of Preoxidized Copper in Aqueous Sulfide Solutions, J. Electrochem. Soc. 154 (2007) C431–C438. doi:10.1149/1.2745647.

[19] J. Chen, Z. Qin, D.W. Shoesmith, Long-term corrosion of copper in a dilute anaerobic sulfide solution, ElectrochimicaActa. 56 (2011) 7854–7861. doi:10.1016/j.electacta.2011.04.086.

[20] G. Kear, B.D. Barker, F.C. Walsh, Electrochemical corrosion of unalloyed copper in chloride media—a critical review, Corros. Sci. 46 (2004) 109–135. doi:10.1016/S0010-938X(02)00257-3.

[21] D.L.A. de Faria, S. Venâncio Silva, M.T. de Oliveira, Raman microspectroscopy of some iron oxides and oxyhydroxides, J. Raman Spectrosc. 28 (1997) 873–878. doi:10.1002/(SICI)1097-4555(199711)28:11<873::AID-JRS177>3.0.CO;2-B.

[22] C. Rémazeilles, P. Refait, On the formation of β-FeOOH (akaganéite) in chloride-containing environments, Corros. Sci. 49 (2007) 844–857. doi:10.1016/j.corsci.2006.06.003.